

Research Article

Insights Into The Carcinogenic Effect of Key Skin Care Ingredients Leading To Breast Cancer: An In-Silico Study

Perna Kadam¹, Sangeeta Sinha^{1*}, Akshita Puri^{2*}

¹ Department of Zoology, Nowrosjee Wadia College, Pune University, India

² P.G.T.D. Zoology, R.T.M Nagpur University, Nagpur, India

Article history:

Submission April 2023

Revised May 2023

Accepted June 2023

**Corresponding author:*

E-mail: sangeeta.amma@gmail.com

akshita.du@gmail.com

ABSTRACT

Breast cancer is the most common form of cancer among all others, prevalent in terms of incidence rates. There is malignancy risk associated with common skin-care ingredients. This study elucidated possible hub genes related to breast cancer provoked by the effect of various chemicals in skin care formulations which were screened through literature. Aluminum chloride, Aluminum chlorohydrate, Dibutyl phthalate, Diethyl phthalate, Di-2-Ethylhexyl phthalate, methylparaben, propylparaben, Triclosan, octamethylcyclotetrasiloxane (D4), and decamethylcyclopentasiloxane (D5) are the 10 chemicals investigated. Xenoestrogens mimic estrogen and interfere with the endocrine system and can disrupt natural hormone synthesis, secretion, transport, and binding. Pathway enrichment of the genes indicated key pathways that are mostly altered in breast cancer. One of the most significant pathways common to almost 7 chemicals is endocrine disruption validating its xenoestrogenic effect while other 3 alter pathways inducing carcinogenic effect. Taken together, the identification of hub genes, pathway enrichment and literature evidence helped to build a correlation between the chemicals and breast cancer. Further analysis of docking studies revealed that AKT1 for aluminum chloride, ESR1 for aluminum chlorohydrate and dibutyl phthalate, PTGS2 and AR for diethyl phthalate, AKT1 for di-2-ethylhexyl phthalate, PGR for methylparaben, AR and PGR for propylparaben, MMP9 for triclosan and CHEK1 for both decamethylcyclopentasiloxane and octamethylcyclotetrasiloxane has shown greater binding affinity highlighting the significance of these proteins and the potential carcinogenic effect of the skin care ingredients under investigation in this study leading to breast cancer.

Keywords: Breast cancer; Skincare ingredients; Bioinformatics; Docking; Endocrine disruptors; Hub

Introduction

Breast cancer (BC) is the most common form of cancer as of 2020, based on data from GLOBOCAN (<https://gco.iarc.fr/>). Among all cancer subtypes, BC has the highest incidence rate (47.8% per 1000000 ASR). Male breast cancers (MBC), which are extremely uncommon, account for roughly 1% of all carcinoma cases. Less breast tissue or hormonal variations may be the cause of MBC's rarity¹. There has been a redistribution in the topology of BC. Most tumors located in the

breast's upper outer quadrant can be caused by either dense epithelial tissue present in females or the use of cosmetics prevailing in that region⁴.

The global skincare market is growing at a rapid rate because of the demand of an ever-increasing population. Endocrine disruptors (EDs) are chemicals that interfere with the endocrine system and can disrupt natural hormone synthesis, secretion, transport, and binding². EDs contribute to the development and spread of existing breast cancers in addition to raising the risk of

How to cite:

Kadam, P., Sinha, S., Puri, A. (2023). Insights Into The Carcinogenic Effect of Key Skin Care Ingredients Leading To Breast Cancer: An In-Silico Study. *Bioinformatics and Biomedical Research Journal* 6 (1): 1 - 20. doi: 10.11594/bbrj.06.01.01

carcinogenesis. Most of the skin care chemicals behave in an endocrine disruption pattern, increasing the risk of breast cancer. By interacting with hormone receptors, they imitate and obstruct endocrine pathways².

Due to their antiperspirant effect, aluminum salts are present in higher concentrations in antiperspirants³. It blocks sweat by plugging the glands and hence is widely used^{3,5}. Not only in an antiperspirant, but aluminum also used in other skincare products such as make-up, creams, etc. It accumulates in the upper outer quadrant, the most prevalent area of BC, at a higher concentration compared to the inner quadrant^{3, 5}. Aluminum is absorbed through the skin, and significant amounts of the metal have been found in breast tissue, nipple aspirate fluid, breast cyst fluids, and milk⁶. Phthalates are esters of phthalic acid that form a key ingredient in many skin care products, as it is a plasticizer. Dibutyl phthalate (DBP), di-2-ethyl-hexyl phthalate (DEHP) and diethyl phthalate (DEP) commonly found in hair cosmetics, deodorants, nail paints, and lotions. DEHP is the most used phthalate in personal hygiene products⁷. The ability of some phthalates to dysregulate steroidogenesis has been demonstrated in studies, and they are thus classified as EDs^{7, 2}. Phthalate inhibits cell-to-cell communication and apoptosis, both of which promote tumor cell proliferation.

Parabens are antimicrobial agents derived from p-hydroxybenzoic acid, with antibacterial effectiveness increasing with the length of the alkyl grouping⁸. Owing to its anti-microbial activity, they are widely used in deodorants, Methyl paraben and propyl paraben have been extensively used in the formulation of body care products including lotions, deodorants^{9, 8}. The presence of penetration enhancers, volatile solvents like acetone and ethanol in cosmetic preparations can affect parabens absorption and increase penetration^{10, 11}. Its absorption is also highly enhanced by skin integrity and barrier function. Because parabens with shorter side chains penetrate the skin better, methylparaben has been demonstrated to be absorbed at a faster rate than other parabens¹¹. Methylparaben was found to be unmetabolized and modestly persistent in the stratum corneum, which may affect keratinocyte differentiation and aging, influencing paraben absorption due to decreased skin integrity and barrier function¹¹. Because of its broad spectral antibacterial

activity on both gram-positive and gram-negative bacteria, triclosan (5-chloro-2-(2,4-dichlorophenoxy) phenol) is commonly employed in a deodorant formulation¹². Triclosan is also found in shampoos, soaps, creams, lotions, and toothpastes. It has a strong affinity for biological systems and accumulates in nonpolar and fatty tissues because it is a stable and fat-soluble molecule¹². Cyclic volatile methyl siloxanes (cVMS) are used as cosmetic additives in skin care products and are soluble in organic solvents. Two of the most used cyclomethicones in skin care formulations are octamethylcyclotetrasiloxane (D4) and decamethylcyclopentasiloxane (D5). They are used as an emollient in shampoos, facial and body lotions and hair conditioners. D4 and D5 are also extremely persistent substances that cause bioaccumulation¹³.

Thus, this data has the potential to focus research on skin care formulations and their impacts due to their bioaccumulation and penetration, which can result in breast cancer. This study uses in-silico analysis to examine the binding affinities of the 10 skincare ingredients linked to breast cancer in order to assess their role in the disease and make comments on the altered genes and their mode of action.

Methods

Screening major skin care ingredients and Network analysis (CTD):

Major skin care ingredients were screened through literature represented in Supplementary Table 1. Further Comparative Toxicogenomics Database (CTD) (<http://ctdbase.org/>) was used to extract link of these chemicals with cancer. In CTD search tool, 10 chemicals were searched that included (CTD accession identifier): aluminum chloride (D000077410) and aluminum chlorohydrate (C016976), dibutyl phthalate (D003993), di-2-ethyl-hexyl phthalate (D004051), and diethyl phthalate (C007379), methylparaben (C015358) and propylparaben (C006068), triclosan (D014260), Cyclic volatile methylsiloxanes (cVMS) like octamethylcyclotetrasiloxane (C024064) and decamethylcyclopentasiloxane (C114768). Chemical-disease relationship was established by sorting cancer category in the disease section and extracting the data for BC in all associations, including curated and inferred data. KEGG and Reactome integrated pathway analysis in CTD was performed to find enriched pathways

of the genes tabulated with the recommended corrected p-value threshold 0.01.

Protein-protein Interaction and hub gene identification:

The genes taken from CTD were then mapped into the online Search Tool for the Retrieval of Interacting Genes (STRING version 11.5) (<https://string-db.org/>) to evaluate relationship among the nodes. The interaction was restricted to Homo sapiens. Interaction with a medium confidence score of 0.4 was considered significant¹⁴. Cytoscape software (version 3.9.1) (<https://cytoscape.org/>) was used to visualize the PPI (Protein-Protein Interaction) network. CytoHubba a tool in Cytoscape, was used to locate hub genes. As any one algorithm does not depict the essential genes¹⁵, the integration of two algorithms Maximal Clique Centrality (MCC) and Degree were used to obtain hub genes¹⁶. In this study, the top 10 genes were taken from these algorithms for larger interactions while top 3 genes were taken for interactions smaller than 10 nodes. Verification of overlapping hub genes was done by Venn diagram. (<https://bioinformatics.psb.ugent.be/webtools/Venn/>).

Molecular docking by Autodock:

Autodock4.2.6 (<https://autodock.scripps.edu/>) is the docking software used to perform this study. The 10 compounds used for docking tests had their 3D ligand structures collected from the PubChem database (<https://pubchem.ncbi.nlm.nih.gov/>), whereas chemicals without 3D structures were sketched in Chemdraw. The 3D structures of proteins were retrieved from Protein Data Bank (<https://www.rcsb.org/>) in '.pdb' format. Ligands and proteins were prepared. Active site determination was done with the help of CastP. Blind docking was performed for some proteins with no active site in CastP. Binding energies were noted. Visualization and analysis were performed in Discovery Studio Visualizer (DSV4.0).

Result and Discussion

This study investigated breast cancer associated with skincare ingredients and its impact. According to some studies, tissues of breast cancer patients contain higher levels of transition metals. Several contradictory studies have found that certain every day-use product, including cosmetic

components, may be linked to breast cancer⁸. Our data suggests the following outcome.

Comparative Toxicogenomics Database:

Thirty-seven and five genes were found for AICI3 and ACH (Table 1). The thirty seven genes for AICI3 were enriched for 146 pathways. The top five pathways included pathways in cancer, hepatitis B, apoptosis, IL-17 signaling pathway and endocrine resistance. While the five genes of ACH were enriched in fifteen pathways. Top five included the endocrine resistance, EGFR tyrosine kinase inhibitor resistance, nuclear signaling by ERBB4, apoptosis – multiple species and signaling by ERBB4 (Fig.1a,b). The two aluminum salts share enriched pathways of endocrine resistance and apoptotic routes, showing their important interplay in these processes. Both these pathways play a leading role in BC through cancer progression¹⁸ and the effect of xenoestrogens^{5, 17}.

Phthalates are extensively studied group with DBP ranking first with 239 genes followed by DEHP with 228. DEP has the lowest data of 33 genes in the phthalate group (Table 1). The 239 genes in DBP were enriched for 273 pathways. Top 5 pathways included pathways in cancer, breast cancer, endocrine resistance, signal transduction and microRNAs in cancer. Two hundred and twenty eight genes in DEHP were enriched for 277 pathways. Top 5 pathways included pathways in cancer, hepatitis B, endocrine resistance, ovarian steroidogenesis and IL-17 signaling pathway. Thirty three genes of diethyl phthalate were enriched for 57 pathways. Pathways in cancer, endocrine resistance, breast cancer, microRNAs in cancer and signal transduction (Fig.1c,d,e). The common enhanced pathway in all three phthalates that potentially directs phthalate action is pathways in cancer and endocrine resistance.

Methylparaben and propylparaben have been studied moderately owing to their set of genes extracted, 37 and 33 genes respectively (Table 1). The 37 genes of methylparaben are involved in 28 pathways. Top 5 being endocrine resistance, estrogen signaling pathway, pathways in cancer, generic transcription pathway and signal transduction. While 33 genes of propylparaben were enriched in 84 pathways. Apoptosis, hepatitis B, endocrine resistance, signal transduction and breast cancer were the top 5 pathways (Fig.2a,b) Endocrine resistance and signal transduction remain common for both parabens indicating the effect of

parabens in these pathways and the effect of parabens both in the signaling cascade and as endocrine disruptors [11, 20].

Triclosan is well studied with 173 genes collected from CTD (Table 1). These genes were enriched in 128 pathways. The top 5 pathways were pathways in cancer, interleukin-4 and 13 signaling, fluid shear stress and atherosclerosis, signal transduction and metabolism (Fig.1f).

cVMS are not well studied as the data consist of fewer number of genes. Almost all genes in the

two classes of cVMS that is D5 and D4 are similar (Table 1). The genes like BRCA1, ATM, BRCA2, CHEK1 and CHEK2 are common in all two. Top 5 pathways showed all common in both cVMS that is DNA Double-Strand break repair, presynaptic phase of homologous DNA pairing and strand exchange, homologous DNA pairing and strand exchange (Fig.2c,d). DNA damage-induced cell cycle checkpoints and HDR through Homologous Recombination.

Table 1. Chemical- disease relationship established from Comparative Toxicogenomics Database.

Chemical	Disease	Genes
Aluminum chloride	Breast neoplasms	37 genes: ACHE AKT1 AR BAX BCL2 BMP2 CASP8 CAT CCND1 CDH1 CLDN1 CTNNB1 DDIT3 ESR2 FOS HRAS IFNG IGF1 IL1B IL6 JUN MKI67 MME MMP9 NFKBIA NOS2 OCLN PTGS2 RAF1 RELA RUNX2 SIRT1 SNAI1 SOD2 TNF TUBB3 VIM
Aluminum chlorohydrate	Breast neoplasms	5 genes: BAX BCL2 ESR1 ESR2 NRG1
Dibutyl phthalate	Breast neoplasms	239 genes: ABCG2 ACTA2 ADAM33 ADAMTS1 ADAR AHR AKAP12 AKT1 ALDOA ANGPTL4 APC2 AR AREG ARHG-DIA ATG10 ATM B4GAT1 BAG1 BAX BCL2 BIRC5 BMP2 BMP4 BRCA1 BRCA2 C1QBP CADM1 CASP7 CASP8 CAT CAV1 CCL20 CCND1 CCNE1 CCNH CD40 CDH1 CDH2 CDKN2A CFL1 CHEK1 CHEK2 CLDN1 CLDN4 CLIC1 COMT CPT1A CRHR1 CTNNB1 CXCL12 CXCL8 CYP17A1 CYP19A1 CYP11A1 CYP11B1 CYP2B1 CYP3A4 DDIT3 DEK DES DHFR DLL4 DNMT1 DNMT3A DNMT3B DPYD EDNRB EEF2 EGF EGFR EIF2S2 EIF6 ELP3 ENO1 EPB41L3 ERBB2 ERBB3 ESR1 ESR2 ESRRB ETS2 ETV4 EXO1 EZH2 F3 FASN FBL FGF10 FGFR1 FGFR2 FHL2 FLNA FOS FOXQ1 GDF10 GJA1 GPER1 GPI GPNMB GPX1 GPX4 GRIK2 GSTP1 H2AX H2BC4 HADHB HES1 HEY1 HEYL HMMR HMOX1 HNRNP R HPSE HSP90AA1 IFNG IGF1 IGF1R IGFBP5 IGFBP7 IL1B IL6 ITS2 JMJD6 JUN KCNH1 KIT KLHDC10 KRT14 KRT18 KRT8 LAMTOR5 LEF1 LEPR LIMD2 LLGL1 LOXL2 LPAR1 MAP3K1 MED28 MEIS1 MFGE8 MIF MIR141 MIR200C MKI67 MMP14 MMP2 MMP9 MRPL19 MT3 MTDH MTO R MYH9 NCOA2 NDRG1 NDUFS3 NECTIN2 NFE2L2 NFKBIA NISCH NOP9 NOTCH1 NOTCH2 NOTCH3 NOTCH4 NQO1 NQO2 NR2F6 NRCAM NRG1 NUDT2 OCLN PABPC1 PARP1 PDE2A PDGFA PER3 PGR PHGDH PIK3CA PLA2G4A PPP1R12B PTEN PTGS2 PTPRD RAD51C RAD54L RAF1 RARA RB1 RELA RGS2 RIC8A RMND1 RPL31 RPS4X RPS6

		RRAD RXRB SER- PINB2 SFRP2 SFRP5 SHMT1 SIRT1 SLC2A2 SLC39A6 SLC5 A5 SNAI1 SNAI2 SOD2 SPP1 SRC SREBF2 STAT3 STC2 S TMN1 STXBP4 SYNJ2 TFAP2A TFRC THBS1 TNF TOP2A TP53 TUBB3 TYMS UBE2C UMPS UPK1B VDR VIM WNT 10B WT1 XRCC2 XRCC3 YAP1 YBX1 ZC3H11A ZEB2
Diethyl phthalate	Breast neo- plasms	33 genes: ABCG2 ADAMTS1 AFP AHR AR BAX BCL2 CASP8 CAT CDKN2A CRHR1 CXCL8 CYP17A1 CYP19A1 CYP1A1 CYP1 B1 CYP2B1 ESR1 ESR2 GPX1 IFNB1 IGF1 IL6 MIR141 M MP14 MMP9 PGR PTGS2 RXRB SER- PINB2 TNF TUBB3 WT1
Di-2-ethyl- hexyl phthalate	Breast neo- plasms	228 genes: ABCB1 ABCB1B ABCG2 ACHE ACTA2 ADAMTS1 AFP AH R AKT1 AKT2 ALDOA ANGPTL4 AR ARHG- DIA ARRDC3 ATM AURKA BAP1 BAX BCHE BCL2 BMP2 BMP4 BTN3A2 CADM1 CASP7 CASP8 CAT CAV1 CCND1 CCNE1 CCNH CD109 CD40 CD74 CDA CDH1 CDH2 CDK N2A CENPF CHEK1 CHEK2 CLDN1 CMC2 COL7A1 COMT COTL1 CPT1A CRHR1 CSF1R CSF2 CST6 CTNNB1 CXCL2 CXCL8 CYP17A1 CYP19A1 CYP1A1 CYP1B1 CYP24A1 CYP 2D6 CYP3A4 DHFR DIO3 DLL1 DNMT1 DNMT3A DNMT3B DPYD DTX3 EDNRB EEF2 EFNA1 EGF EGFR ENO1 EPB 41L3 ERBB2 ERBB3 ESR1 ESR2 ESRR1 ETV4 FABP7 FAS N FGF4 FGFR1 FGFR2 FHL2 FLACC1 FLNA FLT1 FN1 FO S FOXQ1 FST GALNT16 GDF10 GJA1 GPER1 GPX1 GRB7 GRIK2 GSTP1 H2AX H6PD HADHB HES1 HEY1 HEYL H MOX1 HNRNPK HP HRAS HSP90AA1 HSPA1B IDO1 IFNG IGF1 IGF1R IGFBP5 IGFBP7 IL10 IL1B IL6 JAG2 JUN KIT KRT14 KRT18 KRT5 KRT8 LEP LOXL2 LRRC3B MAC1R MAL MDM2 MECOM MIR132 MIR141 MIR146A MIR200B MIR200C MIR221 MIR222 MIR29A MIR345 MIR429 MIR489 MKI67 MME MMP14 MMP2 MMP9 MT3 MTOR MYH9 NC OA1 NDRG1 NFE2L2 NOS2 NOS3 NOTCH1 NOTCH2 NOTC H3 NOTCH4 NQO1 NQO2 NRCAM NRG1 PARP1 PDE2A P DPK1 PDZK1 PER3 PGR PHGDH PIK3CA PPARGC1B PTEN PTGS1 PTGS2 PTHLH RAD51B RALYL RBM3 RELA RPL3 1 RPS4X RPS6 RUNX2 RXRB SER- PINB2 SFRP2 SIRT1 SLC16A3 SLC2A1 SLC2A2 SLCO1B1 S NAI1 SOD2 SPP1 SRC STC2 STXBP4 SULT1A1 SYNJ2 TAF A4 TFPI2 TFRC TGM2 THBS1 TLE3 TNF TOP2A TOX3 TP 53 TRERF1 TRP53 TUBB3 TXN VEGFB VEGFC VIM WNT1 0B WT1 YBX1

Methyl para-ben	Breast neoplasms	37 genes: AKAP12 ATM BAX BCL2 BRIP1 CAT CCND1 CCNE1 CENPF CXCL3 CYP19A1 DHFR EEF2 ELK3 ESR1 ESR2 GPER1 HMOX1 HSP90AA1 HSPA1B IL24 KRT8 LEF1 LEP MKI67 MMP2 NCOA2 NFE2L2 PGR RGS2 RUNX2 SPP1 STMN1 TFAP2A TOP2A UBD VEGFC
Propyl para-ben	Breast neoplasms	33 genes: AR AREG ATM BAX BCL2 BIRC5 CASP7 CASP8 CCND1 CCNE1 CYP19A1 CYP1A1 CYP2B1 E2F1 ESR1 ESR2 FASN FOS GPER1 H2AX HEY1 HP KRT5 LEP MST1 NCOA2 NRG1 PGR SLC2A2 TNF TNFSF10 TP53 TP53BP1
Triclosan	Breast neoplasms	174 genes: ABCB1 ABCC1 ABCG2 ACTA2 ADAM33 ADAMTS1 AFP AHR AKT1 ALDOA ANGPTL4 ANKRD34A APO-BEC3B APRT AR ARTN ATP7B AURKA BAX BCL2 BIRC5 BMP2 BRCA1 CAT CAV1 CCND1 CDH1 CDH2 CDH5 CDKN2A CENPF COMT CPT1A CSF1 CSF2 CST6 CXCL12 CXCL2 CXCR4 CYP17A1 CYP19A1 CYP1A1 CYP1B1 CYP2B1 CYP2D6 CYP3A4 DDIT3 DHFR DKK1 DNMT1 DNMT3B DSC3 EEF2 ENO1 EPB41L3 ESR1 ESR2 ETS2 EXO1 F3 FASN FGF10 FHL2 FLT1 FN1 FOS FST GDF10 GJA1 GPI GPNMB GPX1 GPX4 GRB7 GRIK2 GUCY1A2 H19 HADHB HAPLN4 HES1 HEY2 HEYL HHEX HMOX1 HNRNPK HOXB9 HP HSP90AA1 ICAM5 IGF1 IGF1R IGFBP5 IGFBP7 IL1B IL6 JAG1 JUN KDR KLK10 KRT14 KRT18 LDHB LPAR1 LSP1 MECOM MIF MIR206 MIR429 MKI67 MME MMP2 MMP3 MMP9 MRPS7 MT3 MTOR NCOA2 NDUFS3 NFKBIA NOS2 NOS3 NQO1 NR2F1 NRCAM OCLN PAEP PDE2A PDGFA PER3 PHGDH PPP1R12B PTGS1 PTGS2 RAD51B RARB RELA REPS2 RPL23A RPS6 RRAD RSPO3 RUNX2 SFRP2 SFRP5 SHMT1 SIRT1 SLC16A3 SLC2A1 SLC5A5 SLCO1B1 SNAI1 SNAI2 SOD2 STC2 SULT1A1 TAFA4 TFAP2A TFPI2 TGM2 TNF TNFSF10 TOP2A TOX3 TRIM47 TUBB3 TXN TYMS VEGFC VIM WT1 WWOX XRCC2 YBX1 ZEB1
D5	Breast neoplasms	6 genes: ATM BRCA1 BRCA2 CHEK1 CHEK2 ESR2
D4	Breast neoplasms	7 genes: ATM BRCA1 BRCA2 CHEK1 CHEK2 CYP2B1 ESR1

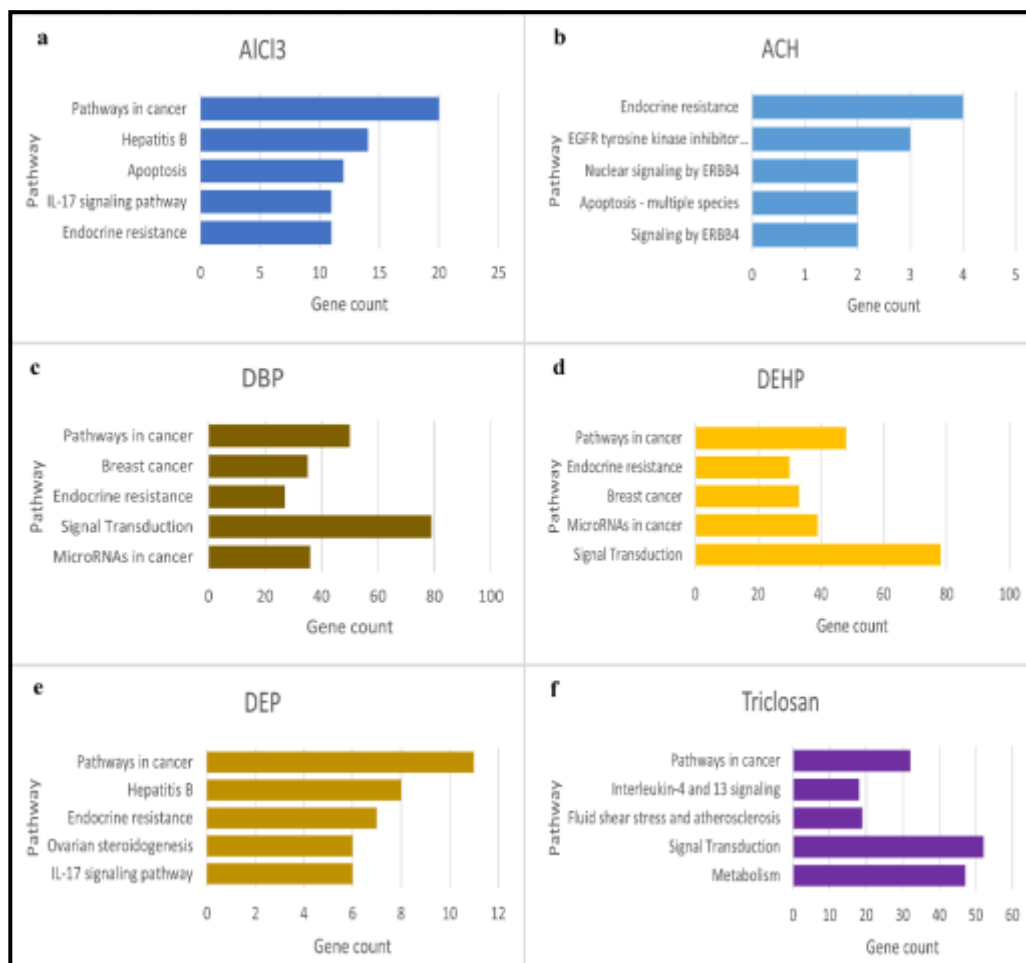


Figure 1. KEGG and Reactome integrated pathway analysis from CTD showing top 5 enriched pathways.

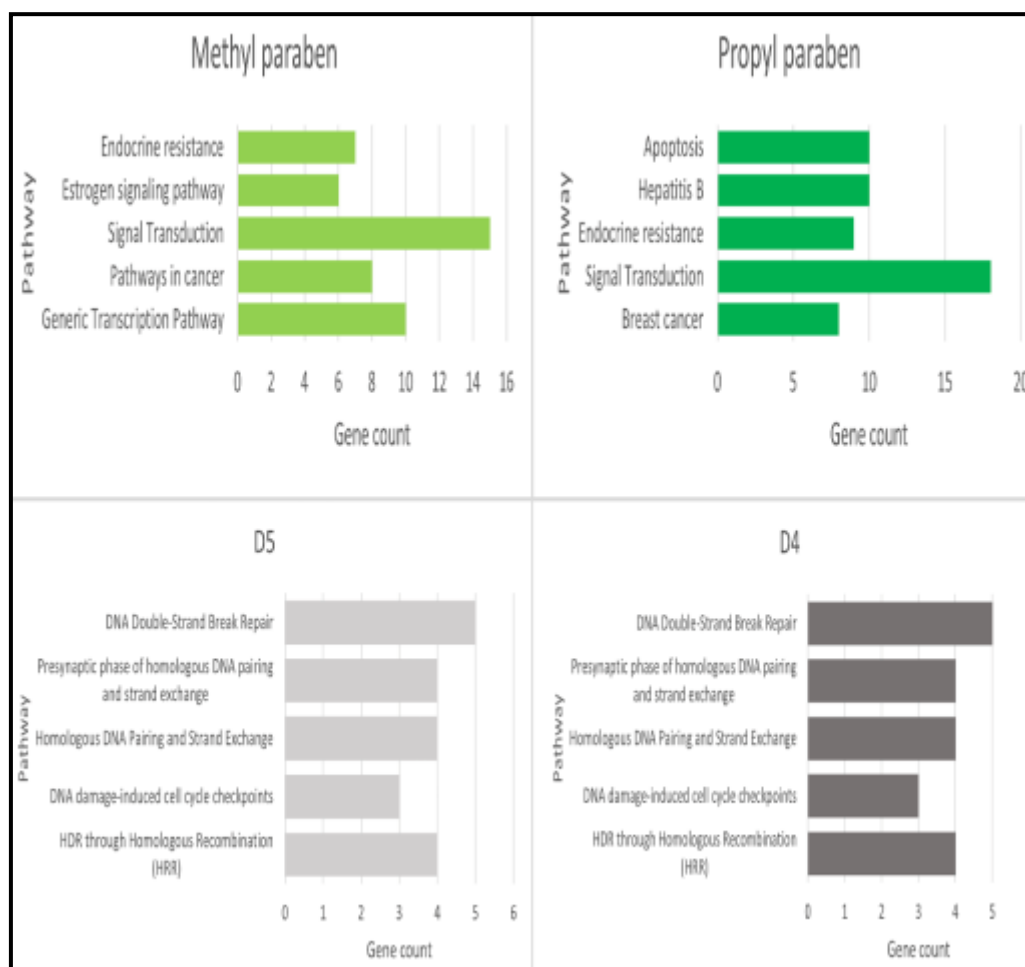


Figure 2. KEGG and Reactome integrated pathway analysis from CTD showing top 5 enriched pathway.

Protein-protein Identification and identification of hub genes:

A total of 37 nodes and 366 edges were involved in the PPI network of genes for AIC13 (Fig.3a). AKT1 was the top gene according to MCC followed by IL6, TNF, MMP9, CTNNB1, JUN, PTGS2, FOS, HRAS and SIRT1. AKT1 also has the highest connectivity degree (33) followed by IL6 (31), TNF (31), MMP4 (30), CTNNB1 (30), PTGS2 (29), JUN (29), IL1B (29), CCND1 (28) and FOS (26). Seven overlapping hub genes were obtained: AKT1, IL6, TNF, CTNNB1, JUN, PTGS2 and FOS (Table 2). Total number of nodes for ACH is 5 as well as edges are 5 (Fig.3b). ESR1 showed the highest degree and MCC value as (3) followed by ESR2 (degree and MCC= 2) and NGR1 (degree and MCC = 2). The 7 hub genes discovered in AIC13 are involved with cell growth and apoptosis, either directly or indirectly. Most of these genes are also located in TNF signaling pathways and breast cancer pathways, implying that

AIC13 may affect these processes, causing progression. In well-established mouse cancer models, aluminum doses comparable to those found in the human breast totally convert cultured mammary epithelial cells, allowing them to form tumors and spread⁶. Based on the findings and the literature reports, AIC13 may appear to act on the invasive phenotype promoting cancer metastasis⁶. ESR1, NGR1, and ESR2 are discovered as hubs in ACH and have been demonstrated to be ligand sensitive. These three genes may be triggered by modifying their binding sites, either chemically by the effect of xenoestrogens or through mutations^{27,31}. This mostly suggests that ACH act as xenoestrogens.

A total of 236 nodes and 3359 edges were involved in the PPI network of genes related to DBP (Fig.3c). Top 10 genes evaluated by MCC are CTNNB1 followed by TP53, STAT3, JUN, AKT1, EGFR, ESR1, PTEN, SRC and MTOR. TP53 shows the highest degree = 145 followed by

AKT1 (138), EGFR (122), CTNNB1 (121), ESR1 (114), CCND1 (105), PTEN (99), JUN (97), ERBB2 (96) and CDH1 (96). Overlapping hub genes in MCC and degree are: PTEN, AKT1, JUN, CTNNB1, ESR1, TP53 and EGFR. (Table 2).

A total of 31 nodes and 171 edges were involved in PPI network of genes related to DEP (Fig.3d). IL6 has the highest MCC score followed by ESR1, PTGS2, TNF, IGF, MMP9, CDKN2A, CASP8, CXCL8 and AR. IL6 was the most outstanding gene with degree= 22 followed by TNF (22), ESR1 (21), PTGS2 (21), AR (27), IGF1 (17), MMP9 (17), CASP8 (16), PGR (16) and CXCL8 (15). Nine overlapping hub genes in these two algorithms are IL6, ESR1, TNF, PTGS2, IGF1, AR, MMP9, CASP8 and CXCL8 (Table 2).

Total number of nodes for DEHP include 216 nodes and 3303 edges (Fig.3e). CTNNB1 has the highest MCC score followed by TP53, JUN, EGFR, AKT, SRC, PTEN, ESR, HRAS and IL6. Amongst them AKT1 showed highest degree= 138 followed by TP53 (133), CTNNB1 (119), ESR1 (115), EGFR (115), CCND1 (104), IL6 (98), TNF (95), PTEN (95) and JUN (95). Overlapping hub genes are eight: PTEN, AKT1, JUN, IL6, CTNNB1, ESR1, TP53 and EGFR (Table 2). Hub genes located in phthalates show overlapping, suggesting a common way of action (Table 2). Hub genes of DBP and DEHP phthalate are similar except the hub IL6, which is present in DEHP. All the hubs obtained in these two phthalates are enriched in the properties of invasion metastasis, cell proliferation and apoptosis. These are the hallmarks of cancer, which signify the action of DBP and DEHP19. However, the hubs found in diethyl phthalate mostly play a role in endocrine receptors, apoptotic processes, and cell communication. This provides a lead on the role of DEP leading to carcinogenicity.

Methylparaben included 37 nodes and 115 edges (Fig.3f). CCND1 has highest score according to MCC followed by ESR1, HSP90AA1, MMP2, LEP, PGR, ATM, CAT, TOP2A and RUNX2. CCND1 also has the highest connectivity degree (25) followed by ESR1 (21), HSP90AA1 (15), PGR (13), TOP2A (11), LEP (11), MMP2 (11), ATM (9), CAT (9) and ESR2 (9). The top ten genes were shown according to MCC and Degree algorithm in Table 2. Nine overlapping hub genes were obtained: CCND1, ESR1,

HSP90AA1, MMP2, LEP, PGR, ATM, CAT and TOP2A.

Propylparaben included 32 nodes and 168 edges (Fig.3g). ESR1 was the top most gene according to MCC followed by TP53, CCND1, TNF, FOS, LEP, AR, CYP19A1, PGR and CASP8. TP53 has the highest connectivity degree (27) followed by ESR1 (25), CCND1 (23), AR (19), TNF (18), CASP8 (16), FOS (15), PGR (14), LEP (14) and ESR2 (12). The top ten genes were shown according to MCC and Degree algorithm in Table 2. Nine overlapping hub genes were obtained: ESR1, TP53, CCND1, TNF, FOS, LEP, AR, PGR and CASP8. Propylparaben contains hubs which can mostly be observed in endocrine disruption by the effect of xenoestrogens. Other hubs contribute to the apoptotic process, while that of methyl paraben are seen mostly in cell proliferation, invasion through the breakage of extracellular barrier and endocrine disruption. This is in accordance with the evidence previously studied on parabens11, 20.

A total of 171 nodes and 1747 edges were involved in PPI network of genes related to Triclosan (Fig.3h). IL6 has highest score according to MCC followed by TNF, FN1, JUN, AKT1, MMP9, ESR1, CCND1, PTGS2 and HSP90AA1. AKT1 has the highest connectivity degree (99) followed by ESR1 (83), TNF (80), IL6 (79), JUN (74), FN1 (71), CCND1 (68), HSP90AA1 (64), MMP9 (62) and CDH1 (62). Nine overlapping hub genes were obtained: IL6, TNF, FN1, JUN, AKT1, MMP9, ESR1, CCND1, and HSP90AA1 (Table 2). Triclosan has a wide variety of hubs extending from endocrine disruptors to cell proliferation and communication.

Six nodes and 11 edges were involved in PPI network of genes related to D5 (Fig.3i). BRCA1 has the highest score according to MCC followed by CHEK2 and CHEK1. BRCA1 has the highest connectivity degree (5) followed by CHEK2 (4), CHEK1 (4). Three overlapping hub genes were: BRCA1, CHEK2 and CHEK1 (Table 2).

Six nodes and 15 edges were involved in D4 (Fig.3j). BRCA1, CHEK1 and ATM had same MCC score. BRCA1, CHEK1 and ATM all have connectivity degree (5). Three overlapping hub genes were: BRCA1, CHEK1 and ATM (Table 2). D4 and D5 contain hubs which are mostly altered in breast cancer and used in DNA repair system. PPI provide a crucial role in understanding interactions between proteins of interest and can help

to deduce key proteins in the network which can potentially be the candidate interacting with the skin care ingredients leading to breast cancer.

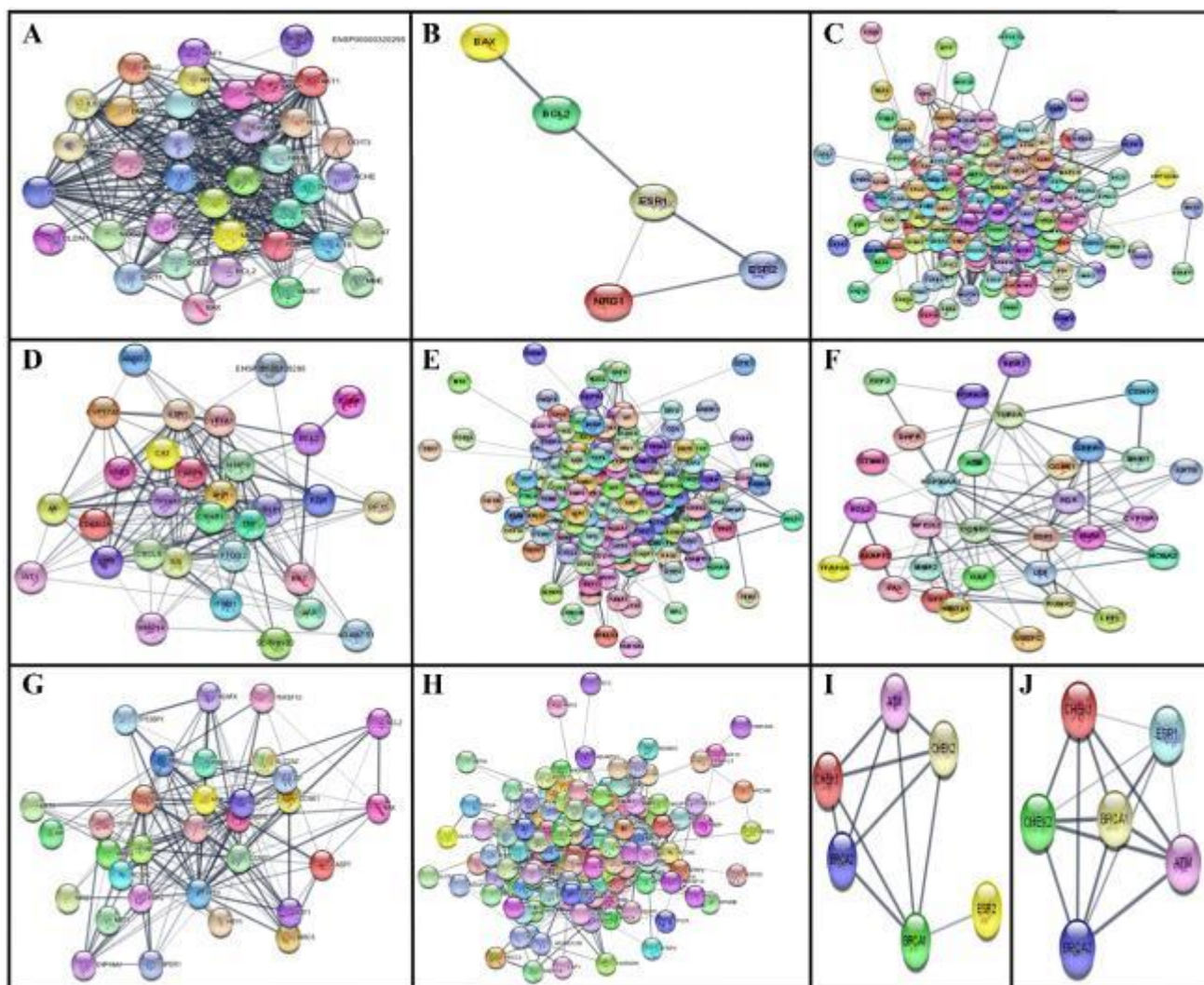


Figure 3. String analysis of genes taken from CTD for particular skin care ingredient and its visualization through Cytoscape.

The nodes are represented by different colors while interactions by lines (edges) which varies in thickness based on the degree of confidence prediction of interaction.

Aluminum chloride (a), Aluminum chlorohydrate (b), Dibutyl Phthalate (c), Diethyl Phthalate (d),

Di-2-ethylhexyl Phthalate (e), Methyl Paraben (f), Propyl Paraben (g), Triclosan (h), Decamethylcyclopentasiloxane (i), Octamethylcyclotetrasiloxane (j).

Table 2: Cytoscape analysis of genes from two algorithms (MCC and Degree) and derivation of overlapping hub genes. Genes placed in MCC and Degree are following increased order of connectivity.

Skin care ingredient	MCC	Degree	Common genes / Hub genes
Aluminum Chloride	AKT1	AKT1	AKT1
	IL6	IL6	IL6
	TNF	TNF	TNF
	MMP9	MMP4	CTNNB1
	CTNNB1	CTNNB1	JUN
	JUN	PTGS2	PTGS2
	PTGS2	JUN	FOS
	FOS	IL1B	
	HRAS	CCND1	
SIRT1	FOS		
Aluminum Chlorohydrate	ESR1	ESR1	ESR1
	NRG1	NRG1	NRG1
	ESR2	ESR2	ESR2
Dibutyl Phthalate	CTNNB1	TP53	CTNNB1
	TP53	AKT1	TP53
	STAT3	EGFR	JUN
	JUN	CTNNB1	AKT1
	AKT1	ESR1	EGFR
	EGFR	CCND1	ESR1
	ESR1	PTEN	PTEN
	PTEN	JUN	
	SRC	ERBB2	
MTOR	CDH1		
Diethyl Phthalate	IL6	IL6	IL6
	ESR1	TNF	ESR1
	PTGS2	ESR1	PTGS2
	TNF	PTGS2	TNF
	IGF1	AR	IGF1
	MMP9	IGF1	MMP9
	CDKN2A	MMP9	CASP8
	CASP8	CASP8	CXCL8
	CXCL8	PGR	AR
AR	CXCL8		
Di-2-ethylhexyl Phthalate	CTNNB1	AKT1	CTNNB1
	TP53	TP53	TP53
	JUN	CTNNB1	JUN
	EGFR	ESR1	EGFR
	AKT1	EGFR	AKT1
	SRC	CCND1	PTEN
	PTEN	IL6	ESR1
	ESR1	TNF	IL6
	HRAS	PTEN	
IL6	JUN		
	CCND1	CCND1	CCND1
	ESR1	ESR1	ESR1
	HSP90AA1	HSP90AA1	HSP90AA1

Methyl paraben	MMP2	PGR	MMP2
	LEP	TOP2A	LEP
	PGR	LEP	PGR
	ATM	MMP2	ATM
	CAT	ATM	CAT
	TOP2A	CAT	TOP2A
	RUNX2	ESR2	
Propyl paraben	ESR1	TP53	ESR1
	TP53	ESR1	TP53
	CCND1	CCND1	CCND1
	TNF	AR	TNF
	FOS	TNF	FOS
	LEP	CASP8	LEP
	AR	FOS	AR
	CYP19A1	PGR	PGR
	PGR	LEP	CASP8
	CASP8	ESR2	
Triclosan	IL6	AKT1	IL6
	TNF	ESR1	TNF
	FN1	TNF	FN1
	JUN	IL6	JUN
	AKT1	JUN	AKT1
	MMP9	FN1	MMP9
	ESR1	CCND1	ESR1
	CCND1	HSP90AA1	CCND1
	PTGS2	MMP9	HSP90AA1
	HSP90AA1	CDH1	
Decamethylcyclotetrasiloxane	BRCA1	BRCA1	BRCA1
	CHEK2	CHEK2	CHEK2
	CHEK1	CHEK1	CHEK1
Octamethylcyclotetrasiloxane	BRCA1	BRCA1	BRCA1
	CHEK1	CHEK1	CHEK1
	ATM	ATM	ATM

Molecular Docking:

Further analysis of the binding affinity with the compound provides evident chemical interaction studies to comment on the function of proteins by the effect of the interaction.

The docking results of 7 hub genes for AIC13 showed that AKT1 has the lowest binding energy i.e., -5.36 kcal/mol (Table 3) indicating high affinity between the protein and the ligand. Although it has no hydrogen bonds it has hydrophobic interactions with Val 83, Phe 161, Leu 181, Leu 295 and Cys 296 whose cumulative effect contributes to the lower binding energy (Fig. 4a). Amongst the 3 hub genes for ACH, ESR1 shows the lowest binding energy (-3.63 kcal/mol) (Table 3). The lowest

binding energy is attributed to the three hydrogen bonds formed with Glu 385, Leu 511 and Ser 512 while there are no hydrophobic interactions (Fig.4b). Increased number of hydrogen bonds has made the interaction of ESR1 and ACH more stable than other proteins.

ESR1 shows the lowest binding energy i.e., -5.48 kcal/mol for the ligand DBP (Table 3). Although it shows no hydrogen bond, the cumulative effect of larger number of hydrophobic interactions like alkyl bond with Leu 384, Ala 350, Leu 540 and Leu 525, Pi alkyl bond with Trp 383, Met 388, Leu 391 and His 524 and Pi-Pi T shaped bond with Phe 404 result in lowering the binding energy thereby stabilizing the interaction (Fig.4c).

Lowest interaction is shown by JUN (-2.97 kcal/mol) and CTNNB1 (-2.37 kcal/mol).

PTGS2 and AR both show the lowest binding energy and hence greatest affinity of -6.94 kcal/mol for the ligand DEP amongst the 9 hub genes (Table 3). PTGS2 shows five hydrogen bonds consisting of two Conventional hydrogen bonds with Gln 462, Carbon hydrogen bond with Pro 155, His 39 and Pi donor hydrogen bond with Cys 47 (Fig.4d). In addition to this, it shows hydrophobic interactions like Pi alkyl bond with Val 47, Pro 154, His 39, Cys 47 and Alkyl bond with Pro 154 and Pro 157. All this contributes to a strong interaction resulting in lowering the binding energy. In contrast, AR shows no hydrogen bonds but shows multiple hydrophobic interaction like Alkyl bonding with Leu 707, Val 746, Met 745, Met 787, Met 749, Leu 973, two Pi alkyl bonds with Phe 764 and one with Leu 704 (Fig.4e). These interactions make the protein-ligand i.e., AR and diethyl phthalate stronger.

Among the 8 hub genes, the lowest binding energy of -4.78 kcal/mol is shown by AKT1 for the ligand DEHP (Table 3). This interaction is due to one hydrogen bond with Glu 17 residue and other hydrophobic interactions like Pi alkyl with Tyr 272, Arg 273, and alkyl bond with Cys 296, Pi anion both with Glu 17 and Pi cation bond with Arg 273 (Fig.4f).

Higher binding affinity has been identified for PGR with Methylparaben (Fig.4g). The lowest binding energy (-4.76 kcal/mol) with PGR is due to hydrogen bonds with Gln 725, Met 759 and Arg 766 (Table 3). While other hydrophobic like Pi T shaped bond with Phe 778, Mi sulphur bond with Met 759, Pi alkyl both with Leu 763 and Alkyl bond with Leu 718 and Met 759 contribute to make the interaction strong and hence lowering the binding energy.

AR and PGR displayed lowest binding energy, -5.31 kcal/mol and -5.30 kcal/mol respectively with propylparaben (Table 3). AR shows lowest binding energy due to two H- bonds with Gln 711, Arg 752 residue and other hydrophobic interactions like Pi sulphur bond with Met 745, Pi sigma bond with Met 745, Pi Pi T shaped bond with Phe 764, Pi alkyl bond with Leu 707, Met 749 and Alkyl bond with Met 895 (Fig.4h). While PGR binding score is also due to two H-bonds with Gln 725, Arg 766 residues and other interactions like Pi sulphur with Met 759, Pi Pi T shaped bond with Phe 778, Pi alkyl bond with Leu 763

and Alkyl bond with Leu 797, Met 801 and Leu 887 (Fig.4i).

Triclosan has the lowest binding energy with MMP9 (-7.24 kcal/mol) (Table 3). The strongest interaction with MMP9 is due to one H- bond with Leu 397 and other interactions like Pi cation with His 401 residue, Pi Pi stalked interaction with His 401, Pi alkyl bond with Leu 418, Arg 424, Val 398 and Alkyl interaction with Arg 424 and Leu 188 (Fig.4j). Lower bonding is seen with HSP90AA1 (-4.76 kcal/mol), IL6 (-4.37 kcal/mol) and JUN (-4.06 kcal/mol). All of which interact with less number of residues.

CHEK1 has the lowest binding energy (-7.40 kcal/mol) (Table 3) and greatest affinity to D5. One hydrogen bond with Ser 147 is observed while four alkyl bonds with Val 23, three alkyl bonds with Leu 84 and Leu 137, two alkyl bonds with Leu 15 and one alkyl bond with Ala 36, Lys 38 and Val 68 contribute to its greater affinity (Fig.4k). CHEK1 shows lowest binding energy (-7.34 kcal/mol) exhibiting greater affinity with ligand D4. It has one H-bond with Cys 48 residue while a number of hydrophobic interactions like Pi sigma bonding with Tyr 20, Pi alkyl bond with Tyr 20, four alkyl bonds with Val 40, two alkyl bonds with Cys 48 and one alkyl bond each with Ile 52, Met 42 and Arg 44 (Fig.4l).

Hence, we found that AKT1 interacted most with AlCl₃ and DEHP. AKT1 α serine-threonine protein kinase that is phosphorylated by phosphoinositide-3kinase (PI3K). AKT1 is one of the most frequently activated protein kinases and is thus classified as an oncogene^{21, 22}. Its activation is linked to apoptosis resistance, increased cell growth and proliferation^{21, 22}. In vivo studies have also been reported of activation of AKT by phosphorylation by the exposure of DEHP²³. Long-term exposure to aluminum transforms human epithelial cells into tumor-forming cells that metastasize⁶. Through the PI3K signaling pathway, AKT is implicated in several stages of tumor formation²⁴. The PI3K/AKT signaling pathway is critical for tumor cell survival¹⁸. Upregulation of AKT1 via the PI3K pathway can be induced by AlCl₃ and or DEHP thereby promoting proliferation and inhibiting apoptosis.

Among the screened proteins against ACH, ESR1 with the binding energy of -3.63 kcal/mol showed the most potent binding. ESR1 also showed the lowest binding energy with DBP (-5.48 kcal/mol). ESR1's activity is crucial in breast

tissue due to the production of essential hormones and hence, binding of other compounds causes its activation, which may lead to ER⁺ tumors^{25, 26}. The ER α , which is encoded by the ESR1 gene, is expressed in roughly 70% of all BC²⁵. ER α has also been demonstrated to play a significant role in metastasis. Few experimental data suggest a link between aluminum chlorohydrate and increased ER α levels²⁷. Hence, ACH and DBP can have carcinogenic effects by activating ESR1 causing constitutive activity of the ER.

PTGS2 and AR have the lowest binding energy of -6.94 kcal/mol with DEP. The cyclooxygenase-2 (COX-2) enzyme is encoded by prostaglandin-endoperoxide synthase 2 (PTGS2), which is involved in inflammation and has been linked to BC²⁸. In BC, cyclooxygenase-2 increases tumor development, invasion, and metastasis²⁹. Propylparaben also shows the lowest binding energy (-5.31 kcal/mol) with AR. In normal breast tissue, androgen receptor (AR) signaling has an antiestrogenic, growth-inhibitory effect. AR's action is also linked to the EF and HER2 signaling pathways. AR binds to the ERES when its expression level is higher than that of the ER, inhibiting cell growth³⁰. AR binding is mostly concerned with endocrine disruption. Hence, DEP can act by disrupting the endocrine function and further take part in metastasis.

PGR binds with methylparaben and shows most stable binding with the lowest binding score of -4.76 kcal/mol. The expression of PGR has also been found as a prognostic marker for BC. Majority of postmenopausal women express estrogen or progesterone-driven breast cancers ³¹. It also binds with propylparaben with binding energy of -5.30 kcal/mol. As the development and progression of BC depend upon hormones like estrogen and progesterone, the action of PGR and ER receptors binding and its activation by other compounds can be performed³². Hence, Methyl paraben and propylparaben both can exhibit endocrine disruption by binding to PGR that is in accordance with the pathway enrichment carried out, suggesting a possible way of the action of parabens. Propylparaben thus shows the strongest binding to hormonal receptors of PGR and AR directing its way of action.

Triclosan exhibited the most potent binding with MMP9 from the hub genes with the lowest binding score of -7.34 kcal/mol. MMP-9 serves as a biomarker for various cancers and is associated in cancer metastasis by disrupting the extracellular matrices³³. Triclosan can thus bind to MMP9 and can lead to metastasis. CHEK1 binding to both D5 and D4 has shown greater binding affinity of -7.40 kcal/mol and -7.34 kcal/mol respectively. Both of which form one hydrogen bond and a larger number of hydrophobic interactions. CHEK1, which is a key component in checkpoint signalling have a significant role in breast cancer³⁴. G2/M checkpoint using checkpoint kinase 1 (CHK1) is critically known in DNA damage response³⁴. This result indicates a common method of action of cVMS by targeting the repair system.

In conclusion, all the chemicals studied have had hubs essential for endocrine function, validating its xenoestrogenic properties. Docking studies showed that aluminum chloride and di-2-ethylhexyl phthalate bind to AKT1 causing disruption in PI3K pathway, which is a hallmark of cancer¹⁸.

Aluminum chlorohydrate and Dibutyl phthalate bind to ESR1, thus acting as a xenoestrogen, which is a key factor in breast cancer^{18, 25, 26}. PTGS2, and AR binding to diethyl phthalate indicate endocrine disruption as well as metastasis by the potential carcinogen diethyl phthalate. Diethyl phthalate as well as Dibutyl phthalate show endocrine disruption, whereas di-2-ethylhexyl phthalate functions by disturbing the signaling cascade.

Binding of PGR with methyl paraben and AR and PGR with propylparaben also suggests an endocrine disruption by way of hormones essential for breast cancer progression. MMP9 for triclosan, which causes metastasis and CHEK1 for both decamethylcyclopentasiloxane and octamethylcyclotetrasiloxane, which disrupt the repair system has shown greater binding affinity, revealing the importance of these proteins in breast cancer due to skin care products and thus suggesting a carcinogenic effect of these compounds. Further analysis revealed that the literature studies, pathway enrichment analysis, hub gene identification and docking results coincide with validating our result.

Table 3. Molecular Docking between selected skin care ingredients and overlapping hub genes with lowest binding energy at the top and highlighted with red for every ingredient. Interactions for the same are highlighted red.

Skin care ingredient	Hub gene	Binding energy kcal/mol	Number of Hydrogen bond	Interactions	
				Hydrogen bond	Other interactions
Aluminum chloride	AKT1	-5.36	0	-	Val 83, Phe 161, Leu 181, Leu 295, Cys 296
	PTGS2	-5.16	0	-	Arg 120, Ser 121, Ile 124, Pro 528, Met 535, Phe 371
	TNF	-4.36	0	-	Ala 62, Leu 71, trp 107
	IL6	-4.3	0	-	Tyr 31, Ile 32, Gly 35, Ala 114, Val 115, Ser 118
	CTNNB1	-4.13	0	-	Leu 286, Asn 326, Ile 327, Tyr 331
	JUN	-3.05	0	-	Met 300, Glu 303, Gln 304.
	FOS	-2.8	0	-	Arg 141, Arg 144, Glu 145
Aluminum chlorohydrate	ESR1	-3.63	3	Glu 385, Leu 511, Ser 512	-
	NRG1	-3.49	1	Glu 10	
	ESR2	-3.39	1	Glu 305	-
Dibutyl Phthalate	ESR1	-5.48	0	-	Ala 350, Leu 384, Trp 383, Met 388, Leu 391, Phe 404, His 524, Leu 525, Leu 540
	EGFR	-4.91	3	Cys 751, Thr 830, Asp 831	Val 702, Ala 719, Lys 721, Met 742, Leu 764
	AKT1	-4.9	0	-	Trp 80, Leu 210, Lys 268, Val 270, Asp 292
	PTEN	-4.45	6	His 93, Cys 124, Lys 125, Ala 126, Gly 127, Arg 130	Asp 92, His 93, Lys 125, Ala 126, Lys 128, Gln 171, Gly 189
	TP53	-4	2	Phe 328, Leu 330	Phe 341, Arg 342, Leu 344
	JUN	-2.97	2	Lys 288	Leu 280, Lys 283, Val 284, Lys 285, Lys 288
	CTNNB1	-2.37	2	His 544, Pro 606	Thr 547, Ser 605, Ile 610
Diethyl Phthalate	PTGS2	-6.94	5	His 39, Cys 47, Pro 155, Gln 462	His 39, Val 46, Cys 47, Pro 154, Pro 157
	AR	-6.94	0	-	Leu 704, Leu 707, Met 745, Val 746, Met 749, Phe 764, Met 787, Leu 873
	MMP9	-6.76	6	Ala 189, His 401, Glu 402, His 405, His 411	Leu 187, Leu 188, His 401, Glu 402, His 405, His 411
	ESR1	-6.38	1	Leu 387	Leu 346, Ala 350, Leu 384, Leu 387, Leu 391, Phe 404, Met 421
	IGF1	-6.25	5	Phe 25, Tyr 24, Cys 18	Gln 15, Cys 18, Tyr 24
	TNF	-5.76	3	His 66, Gln 113	His 66, Leu 67

	CASP8	-5.26	4	Thr 4, His 317, Gly 318	Ile 257, His 317, Tyr 324, Cys 360
	CXCL8	-4.9	2	Cys 50, Leu 49	Cys 9, Leu 49
	IL6	-4.67	2	Asn 144	Val 96, Glu 99, Pro 141, Ala 145, Leu 148
Di-2-ethylhexyl Phthalate	AKT1	-4.78	1	Glu 17	Glu 17, Tyr 272, Arg 273, Cys 296
	PTEN	-4.57	0	-	His 93, Lys 125, Ala 126, Lys 128, Arg 130, Ile 168
	TP53	-4.23	0	-	Leu 330, Ile 332, Phe 338, Arg 342
	EGFR	-3.97	1	Arg 807	Ala 674, Ser 744
	ESR1	-3.97	2	Asn 532, Pro 535	Ala 340, Lys 529, Leu 541
	JUN	-3.88	0	-	Arg 276, Arg 279, Leu 280, Lys 283
	IL6	-3.36	0	-	Leu 64, Arg 168
	CTNNB1	-3.08	2	His 544, Pro 606	Pro 606, Ile 610
Methyl para-ben	PGR	-4.76	3	Gln 725, Met 759, Arg 766	Leu 718, Met 759, Leu 763, Phe 778
	CAT	-4.52	3	His 166, Pro 172, Asn 403	His 166, Lys 169, Pro 172, Arg 388, Asp 389
	TOP2A	-4.48	4	Asn 91, Ala 167, Lys 168, Ser 149	Ser 149
	ESR1	-4.37	2	Pro 325, Lys 449	Pro 324, Glu 353, Met 357, Trp 360, Ile 387, Lys 449
	ATM	-4.13	3	Leu 1798, Trp 1805	Leu 1794, Ile 1804
	LEP	-4.01	2	Gln 130, Asn 22	Ile 21, Ile 24, Val 123, Leu 126
	MMP2	-3.92	5	Leu 3, Lys 16, Phe 17	Leu 3, Pro 14, Cys 15, Phe 17
	CCND1	-3.86	3	Cys 73, Gln 183	Cys 68, Pro 79, His 158, Ala 187
	HSP90AA1	-3.57	7	Asn 40, Lys 41, Glu 42, Gln 194, Tyr 197, Arg 202	
Propyl para-ben	AR	-5.31	2	Gln 711, Arg 752	Leu 707, Met 745, Met 749, Phe 764, Met 895
	PGR	-5.3	2	Gln 725, Arg 766	Met 759, Leu 763, Phe 778, Leu 797, Met 801, Leu 887
	ESR1	-4.83	1	Glu 353	Ala 350, Trp 383, Leu 384, Leu 387, Phe 404, Leu 525
	CASP8	-4.62	1	Glu 396	Phe 355, Phe 399, Leu 401
	TNF	-4.19	2	Ala 62, Gln 113	Glu 64, Leu 67
	LEP	-4.13	3	Gly 44, Gln 134, Asp 135	Ile 42, Pro 43
	CCND1	-4.01	2	His 158, Gln 183	Cys 68, Cys 73, Ala 187
	TP53	-3.94	1	Leu 330	Phe 341, Leu 344
FOS	-3.34	1	Glu 175	Leu 172, Lys 176	
	MMP9	-7.24	1	Leu 397	Leu 188, Val 398, His 401, Leu 418, Arg 424
	AKT1	-6.18	0	-	Trp 80, Leu 210, Val 270

Triclosan	FN1	-5.69	1	Thr 44	Asp 30, Arg 46, Asn 47
	ESR1	-5.33	0	-	Glu 323, Pro 324, Ile 326, Leu 327, Glu 353, Met 357, Ile 386
	CCND1	-5.26	0	-	Cys 68, Cys 73, Glu 75, Pro 79, His 158, Gln 183, Ala 187, Thr 184
	TNF	-5.1	2	Gln 82, Cys 96	Cys 96
	HSP90AA1	-4.76	3	Pro 82, Asn 83	Ile 81, Val 92, Lys 185
	IL6	-4.37	1	Pro 141	Glu 95, Val 96, Pro 139
	JUN	-4.06	1	Lys 288	Lys 285, Lys 288
D5	CHEK1	-7.4	1	Ser 147	Leu 15, Val 23, Ala 36, Lys 38, Val 68, Leu 84, Leu 137
	BRCA1	-7.1	0	-	Pro 25, Ile 31, His 41, Ile 42, Leu 63, Phe 79
	CHEK2	-6.75	0	-	Lys 244, Val 246, Lys 289, Leu 303, Met 304
D4	CHEK1	-7.34	1	Cys 48	Tyr 20, Val 40, Met 42, Arg 44, Cys 48, Ile 52
	BRCA1	-6.91	0	-	Ile 21, Pro 25, His 41, Ile 42, Phe 43, Leu 63, Phe 79
	ATM	-6.85	1	Thr 2743	Phe 2265, Lys 2747

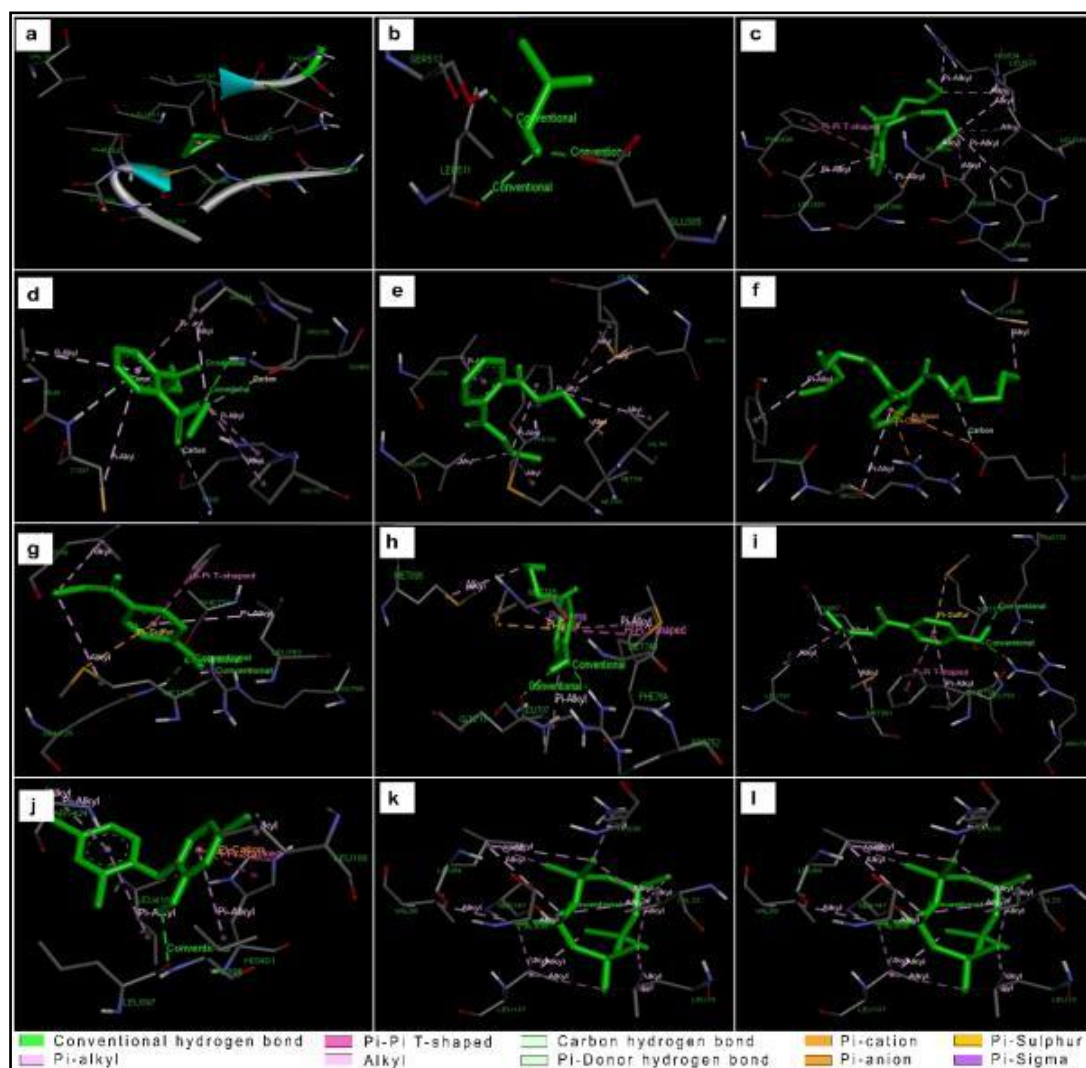


Figure. 4. 3D visualization of docking analysis of lowest binding skin care ingredients (Green colored) with the hub genes (grey and red wire-frame structure).

Interactions are color coded. Aluminum chloride with AKT1 (a), Aluminum chlorohydrate with ESR1 (b), Dibutyl Phthalate with ESR1 (c), Diethyl Phthalate with PTGS2 (d) and AR (e), Di-2-ethylhexyl phthalate with AKT1 (f), Methyl paraben with PGR (g), Propyl paraben with AR (h) and PGR (i), Triclosan with MMP9 (j), Decamethylcyclotrasiloxane i.e D5 with CHEK1 (k) and Octamethylcyclotetrasiloxane i.e D4 with CHEK1 (l).

Conclusion

The present study highlighted that Aluminum chlorohydrate, Dibutyl Phthalate, Diethyl phthalate, Methyl paraben and Propyl paraben show xenoestrogenic behavior by binding to hormonal receptors. In addition, Aluminum chloride, Di-2-ethylhexyl phthalate, triclosan, D4 and D5

disrupt the major signaling cascade which are potential hallmarks of cancer. Through this in-silico analysis significant genes that could be affected by skin care chemicals have been ruled out. Thus, it provides useful insights on targeting assays for toxicity of the altered genes leading to breast cancer. The impacts of skin care products point to the need for more research into molecular interactions and concentration determination for toxicity and disease prevention. Further in vivo studies are envisaged for validating the carcinogenicity of the skin care ingredients and assist in studying the formulations and bioaccumulation factor during development of new skin care products.

Acknowledgments

PK and SS acknowledge the Department of Zoology, Nowrosjee Wadia College, Savitribai

Phule Pune University, Pune, India for their encouragement and support. AP acknowledges the PGTD Zoology RTM Nagpur University for their support.

Declaration of Competing Interests

The authors declare that they have no known competing financial interests or personal relationships that could have appeared to influence the work reported in this paper.

Funding

This research did not receive any specific grant from funding agencies in the public, commercial, or not-for-profit sectors.

References

1. Yalaza, M., Inan, A., & Bozer, M. (2016). Male Breast Cancer. *The journal of breast health*, 12(1), 1–8. <https://doi.org/10.5152/tjbh.2015.2711>
2. Burks, H., Pashos, N., Martin, E., Mclachlan, J., Bunnell, B., & Burow, M. (2017). Endocrine disruptors and the tumor microenvironment: A new paradigm in breast cancer biology. *Molecular and Cellular Endocrinology*, 457. <https://doi.org/10.1016/j.mce.2016.12.010>
3. Klotz, K., Weistenhöfer, W., Neff, F., Hartwig, A., van Thriel, C., & Drexler, H. (2017). The health effects of aluminum exposure. *Deutsches Arzteblatt International*, 114(39). <https://doi.org/10.3238/arztebl.2017.0653>
4. Linhart, C., Talasz, H., Morandi, E. M., Exley, C., Lindner, H. H., Taucher, S., Egle, D., Hubalek, M., Concini, N., & Ulmer, H. (2017). Use of Underarm Cosmetic Products about Risk of Breast Cancer: A Case-Control Study. *EBioMedicine*, 21. <https://doi.org/10.1016/j.ebiom.2017.06.005>
5. Wallace, D. R. (2015). Nanotoxicology and metalloestrogens: Possible involvement in breast cancer. In *Toxics* (Vol. 3, Issue 4). <https://doi.org/10.3390/toxics3040390>
6. Mandriota, S. J., Tenan, M., Ferrari, P., & Sappino, A. P. (2016). Aluminium chloride promotes tumorigenesis and metastasis in normal murine mammary gland epithelial cells. *International Journal of Cancer*, 139(12), 2781–2790. <https://doi.org/10.1002/IJC.30393>
7. Crobbeddu, B., Ferraris, E., Kolasa, E., & Plante, I. (2019). Di(2-ethylhexyl) phthalate (DEHP) increases proliferation of epithelial breast cancer cells through progesterone receptor dysregulation. *Environmental Research*, 173. <https://doi.org/10.1016/j.envres.2019.03.037>
8. Konduracka, E., Krzemieniecki, K., & Gajos, G. (2014). Relationship between everyday use cosmetics and female breast cancer. In *Polskie Archiwum Medycyny Wewnętrznej* (Vol. 124, Issue 5). <https://doi.org/10.20452/pamw.2257>
9. Darbre, P. D., & Harvey, P. W. (2008). Paraben esters: Review of recent studies of endocrine toxicity, absorption, esterase and human exposure, and discussion of potential human health risks. In *Journal of Applied Toxicology* (Vol. 28, Issue 5). <https://doi.org/10.1002/jat.1358>
10. Darbre, P. D., Aljarah, A., Miller, W. R., Coldham, N. G., Sauer, M. J., & Pope, G. S. (2004). Concentrations of Parabens in human breast tumours. *Journal of Applied Toxicology*, 24(1). <https://doi.org/10.1002/jat.958>
11. A.F., F., P.J., F., D.V., B., & J.A., Y. (2019). Paraben Toxicology. *Dermatitis*, 30(1). <https://doi.org/10.1097/der.0000000000000428>
12. Oliveira, E. C. V. de, Salvador, D. S., Holsback, V., Shultz, J. D., Michniak-Kohn, B. B., & Leonardi, G. R. (2021). Deodorants and antiperspirants: identification of new strategies and perspectives to prevent and control malodor and sweat of the body. In *International Journal of Dermatology* (Vol. 60, Issue 5). <https://doi.org/10.1111/ijd.15418>
13. Farasani, A., & Darbre, P. D. (2017). Exposure to cyclic volatile methylsiloxanes (cVMS) causes anchorage-independent growth and reduction of BRCA1 in non-transformed human breast epithelial cells. *Journal of Applied Toxicology*, 37(4). <https://doi.org/10.1002/jat.3378>
14. Bozhilova, L. v., Whitmore, A. v., Wray, J., Reinert, G., & Deane, C. M. (2019). Measuring rank robustness in scored protein interaction networks. *BMC Bioinformatics*, 20(1). <https://doi.org/10.1186/s12859-019-3036-6>
15. del Rio, G., Koschützki, D., & Coello, G. (2009). How to identify essential genes from molecular networks? *BMC Systems Biology*, 3. <https://doi.org/10.1186/1752-0509-3-102>
16. Chin, C. H., Chen, S. H., Wu, H. H., Ho, C. W., Ko, M. T., & Lin, C. Y. (2014). cytoHubba: Identifying hub objects and sub-networks from complex interactome. *BMC Systems Biology*, 8(4). <https://doi.org/10.1186/1752-0509-8-S4-S11>
17. Farasani, A., & Darbre, P. D. (2015). Effects of aluminium chloride and aluminium chlorohydrate on DNA repair in MCF10A immortalised non-transformed human breast epithelial cells. *Journal of Inorganic Biochemistry*, 152. <https://doi.org/10.1016/j.jinorgbio.2015.08.003>
18. Hanahan, D., & Weinberg, R. A. (2011). Ha1. Hanahan D, Weinberg RA. Hallmarks of cancer: The next generation. *Vol. 144, Cell*. 2011. p. 646–74. hallmarks of cancer: The next generation. In *Cell* (Vol. 144, Issue 5). <https://doi.org/https://doi.org/10.1016/j.cell.2011.02.013>
19. Fiocchetti, M., Bastari, G., Cipolletti, M., Leone, S., Acconcia, F., & Marino, M. (2021). The peculiar estrogenicity of diethyl phthalate: Modulation of estrogen receptor α activities in the proliferation of breast cancer cells. *Toxics*, 9(10). <https://doi.org/10.3390/toxics9100237>
20. Darbre, P. D. (2009). Underarm antiperspirants/deodorants and breast cancer. *Breast Cancer Research*, 11(SUPPL. 3). <https://doi.org/10.1186/bcr2424>
21. Liu, H., Radisky, D. C., Nelson, C. M., Zhang, H., Fata, J. E., Roth, R. A., & Bissell, M. J. (2006). Mechanism of Akt1 inhibition of breast cancer cell invasion reveals a protumorigenic role for TSC2. *Proceedings of the National Academy of Sciences of the United States of America*, 103(11). <https://doi.org/10.1073/pnas.0511342103>
22. Ju, X., Katiyar, S., Wang, C., Liu, M., Jiao, X., Li, S., Zhou, J., Turner, J., Lisanti, M. P., Russell, R. G., Mueller, S. C., Ojeifo, J., Chen, W. S., Hay, N., & Pestell, R. G. (2007). Akt1 governs breast cancer progression in vivo. *Proceedings of the National Academy of Sciences of the United States of America*, 104(18). <https://doi.org/10.1073/pnas.0605874104>
23. Ye, H., Ha, M., Yang, M., Yue, P., Xie, Z., & Liu, C. (2017). Di-2-ethylhexyl phthalate disrupts thyroid hormone homeostasis through activating the Ras/Akt/TRHR pathway and inducing hepatic enzymes. *Scientific Reports*, 7. <https://doi.org/10.1038/srep40153>

24. Wu, W., Chen, Y., Huang, L., Li, W., Tao, C., & Shen, H. (2020). Original Article Effects of AKT1 E17K mutation hotspots on the biological behavior of breast cancer cells. *Int J Clin Exp Pathol*, 13(3).
25. Haque, M. M., & Desai, K. v. (2019). Pathways to Endocrine Therapy Resistance in Breast Cancer. In *Frontiers in Endocrinology* (Vol. 10). <https://doi.org/10.3389/fendo.2019.00573>
26. Saha Roy, S., & Vadlamudi, R. K. (2012). Role of Estrogen Receptor Signaling in Breast Cancer Metastasis. *International Journal of Breast Cancer*, 2012. <https://doi.org/10.1155/2012/654698>
27. Gorgogietas, V. A., Tsialtas, I., Sotiriou, N., Laschou, V. C., Karra, A. G., Leonidas, D. D., Chrousos, G. P., Protopapa, E., & Psarra, A.-M. G. (2018). Potential interference of aluminum chlorohydrate with estrogen receptor signaling in breast cancer cells HHS Public Access. In *J Mol Biochem* (Vol. 7, Issue 1). PMID: 30148119; PMCID: PMC6108589.
28. Gao, J., Ke, Q., Ma, H. X., Wang, Y., Zhou, Y., Hu, Z. bin, Zhai, X. J., Wang, X. C., Qing, J. W., Chen, W. sen, Jin, G. F., Liu, J. Y., Tan, Y. F., Wang, X. R., & Shen, H. B. (2007). Functional polymorphisms in the cyclooxygenase 2 (COX-2) gene and risk of breast cancer in a Chinese population. *Journal of Toxicology and Environmental Health - Part A: Current Issues*, 70(11). <https://doi.org/10.1080/15287390701289966>
29. Saindane, M., Rallabandi, H. R., Park, K. S., Heil, A., Nam, S. E., Yoo, Y. B., Yang, J. H., & Yun, I. J. (2020). Prognostic Significance of Prostaglandin-Endoperoxide Synthase-2 Expressions in Human Breast Carcinoma: A Multiomic Approach. *Cancer Informatics*, 19. <https://doi.org/10.1177/1176935120969696>
30. Chen, M., Yang, Y., Xu, K., Li, L., Huang, J., & Qiu, F. (2020). Androgen Receptor in Breast Cancer: From Bench to Bedside. In *Frontiers in Endocrinology* (Vol. 11). <https://doi.org/10.3389/fendo.2020.00573>
31. Gaudet, M. M., Campan, M., Figueroa, J. D., Yang, X. R., Lissowska, J., Peplonska, B., Brinton, L. A., Rimm, D. L., Laird, P. W., Garcia-Closas, M., & Sherman, M. (2009). DNA hypermethylation of ESR1 and PGR in breast cancer: Pathologic and epidemiologic associations. *Cancer Epidemiology Biomarkers and Prevention*, 18(11). <https://doi.org/10.1158/1055-9965.EPI-09-0678>
32. Horwitz, K. B., & McGuire, W. L. (1978). Estrogen control of progesterone receptor in human breast cancer. Correlation with nuclear processing of estrogen receptor. *Journal of Biological Chemistry*, 253(7). [https://doi.org/10.1016/s0021-9258\(17\)38062-6](https://doi.org/10.1016/s0021-9258(17)38062-6)
33. Huang, H. (2018). Matrix metalloproteinase-9 (MMP-9) as a cancer biomarker and MMP-9 biosensors: Recent advances. In *Sensors (Switzerland)* (Vol. 18, Issue 10). <https://doi.org/10.3390/s18103249>
34. Al-Kaabi, M. M., Alshareeda, A. T., Jerjees, D. A., Muf-tah, A. A., Green, A. R., Alsubhi, N. H., Nolan, C. C., Chan, S., Cornford, E., Madhusudan, S., Ellis, I. O., & Rakha, E. A. (2015). Checkpoint kinase1 (CHK1) is an important biomarker in breast cancer having a role in chemotherapy response. *British Journal of Cancer*, 112(5). <https://doi.org/10.1038/bjc.2014.576>